Submitted to: American Vacuum Society 1991 38th National Symposium
November 11-15, 1991

BNL--46994

DE92 007171

PHOTODESORPTION FROM COPPER, BERYLLIUM AND THIN FILMS*

C. L. Foerster, H. J. Halama and G. Korn

Brookhaven National Laboratory, NSLS - Bldg. 725C

Upton, New York 11973

ABSTRACT

Ever increasing circulating currents in electron-positron colliders and light sources demand lower and lower photodesportion (PSD) from the surfaces of their vacuum chambers and their photon absorbers. This is particularly important in compact electron storage rings and B meson factories where photon power of several kW cm^{-1} is deposited on the surfaces. Given the above factors we have measured PSD from 1*m* long bars of (a) solid copper and solid beryllium, and (b), TiN, Au and C thin films deposited on solid copper bars. Each sample was exposed to about 10^{23} photons/*m* with a critical energy of 500 eV at the VUV ring of the NSLS. PSD was recorded for two conditions: after a 200°C bake-out and after an Ar glow discharge cleaning. In addition, we also measured reflected photons, photoelectrons and desorption as functions of normal, 75 mrad, 100 mrad, and 125 mrad incident photons.

*Work performed under the auspices of U.S. DOE under contract DE-AC02-76CH00016.

I. INTRODUCTION

Since the gas load in electron storage rings is dominated by photon stimulated desorption, PSD influences the design, cost and performance of these machines. Desorption and the accompanying heat dissipation become more critical with increasing beam current and decreasing bending radius. Several machines either proposed (B and Φ factories), or under construction, (compact rings for X-ray lithography) are strongly influenced by the above two parameters.

We have therefore undertaken extensive studies aimed at identifying vacuum chamber materials with good mechanical properties, high thermal conductivity, and low photo-desorption. Our investigation was guided by the following considerations:

1) photoelectron production, since surface gases are desorbed by photoelectrons [1-4].

2) surfaces with low adsorption which are easily cleaned.

3) angle of incidence and reflectivity[3,5].

It is hoped that the information presented can serve as a starting point for the design of storage ring vacuum systems and predict their performance in terms of conditioning time and beam lifetime. The two commonly used metals, stainless steel and aluminum are not discussed due to their low thermal conductivity and high initial PSD respectively. Ample data on these metals can be found in published literature[2,3,5,6,7]. A sample of hot rolled 304 stainless steel was run for reference.

II. Experimental Considerations

The experimental set-up was constructed to execute the following tasks and to yield the following quantities:

a) 200°C bake-out

b) possibility of in-situ glow discharge

c) calibration of the RGA and gas conductance

d) incident and reflected photons obtained by measuring photoelectron collected on insulated electrodes when either positive or negative voltages are applied to them.

e) desorption coefficient, η and integrated gas load as a function of dose[2].

A. Experimental Apparatus

The experimental chamber, depicted in Fig. 1, is connected through long bellows to the U10B beam line, at the NSLS;[2,8] so that the angle of incident photons on the metal test bar, can be adjusted. The opening aperture limits the white photon beam, having a critical energy of 500eV, to 10 mrad horizontally and 3.8 mrad vertically, yielding a cut-off energy (FWHM) of 22eV. This limit is primarily imposed by gas conductance necessary for η calculations. Variable voltage power supplies are connected to the wire, and copper end plate, thus permitting measurements of both absorbed and reflected photons depending on polarity used. Before every experimental run the entire system is baked for several days at 200°C and the RGA is calibrated for H_2 CO and CO_2.

B. Measurements

Since photoelectron production[3,9] for a given metal can be calculated from the absorbed photon flux[3] and since the desorption for a given surface condition depends on photoelectrons[2,4], the desorption yields and photoelectrons are measured simutaneously. Initially, photocurrent produced in the end plate (in Fig 1) by photons at normal incidence is obtained using negative

and positive polarity. Due to the small end plate area exposed to light as compared to the total area of the apparatus, accurate desorption yield cannot be measured. Once the above measurement is completed the experimental chamber is rotated horizontally so that the incident photons strike the sample bar at 100 mrad. Pressure rises($\Delta P/P$) for the gases of interest, i.e., H^2, CH^4, CO and CO^2, are obtained from calibrated BAG and RGA readings and the respective yields in molecules per photon are calculated[2]. In order to follow the established conventions, total photon flux is used in the PSD calculations. However, when comparing our results with others an appropriate correction for our vertical aperture must be made. Along with the PSD measurements, absorbed and reflected photons are measured by biasing the wire and the end plate stop.

During the course of this experiment we have investigated the following bars with surface area of (122 x 5)cm^2:

1. OFHC copper
2. OFHC copper + TiN film 2.5 μ m thick
3. OFHC copper plated with 1.3 μ m of gold
4. OFHC copper + " carbonic" film deposited using RF assisted glow discharge[10,11] and a mixture of $3CH_4$ and 97% H^2. The bar had to be coated with TiN(3) to achieve good carbon adhesion. The resulting 1200 A° thick film[12] was clear and transparent with roughness of 150 A°.
5. OFHC copper machined to a sawtooth finish, in order to intercept the photons at normal incidence.
6. same as (5) + plated with 1.3 μ m of gold
7. Beryllium

8. Hot rolled 304 stainless steel (dull finish)

Each of the above samples was investigated for 2 surface conditions:

a) after an in-situ bake at 200°C for at least several days to simulate a newly constructed accelerator

b) after an in-situ Argon glow discharge cleaning[13] initiated at a photon dose of ~ 10^{22} photons. The sample was subjected to 2 x 10^{18} ions/cm^2 at a temperature of 200°C followed by an additional one day bake to elliminate the inbedded Ar[12]. This treatment yields the lowest η but cannot easily be implemented in storage rings.

Only sample 3 obtained an additional treatment, namely glow discharge in a separate vacuum system using the same parameters as (b). It was then transferred in air to the U10B set-up as is commonly done at the NSLS[14] and measured after bake (a). Exposure to atmosphere was approximately 24 hours following a nitrogen backfill.

Finally PSD and photoelectron production were measured as a function of 3 different angles of incidence (75, 100 and 125 mrad).

III. Results

A. Photoelectron Production

Normal incidence photons

Since gas desorption is mediated by photoelectrons[2-4] a meaningful study of this phenomenon must include photoelectron production which can be calculated from synchrotron radiation spectra and photo-electric quantum efficiencies. For this experiment, the product of photon spectrum[16] and the photoyields[9] integrated over the energy range determined by our

vertical aperture of 3.8 mrad gave the following photoelectron currents in μA per mA of beam per horizontal mrad.

Material	Calculated Current
Aluminum	0.65
Gold	0.53
Carbon	0.24
Copper	0.5

Stainless steel current was estimated from the data[9] on chromium and nickel to be close to that of copper. Photoelectric quantum efficiencies for Berillium were not available.

Since the photon stop is made of copper only the yield for Cu was measured giving 0.4 μA/mA mrad. The agreement is quite good considering various error sources entering into calculations and measurements. More than 95% of electrons produced had energy lower than 30eV and when the beam stop was grounded, 55% of generated electrons struck the surrounding surfaces.

100 Milliradian Incidence

Adjusting the magnitudes and the polarities of the voltages applied to various components in Fig 1 permits us to measure photoelectrons created by both the absorbed and reflected photons. In this measurement, an electrically isolated ETP copper bar used as a sample yielded the following photoelectric currents due to:

1) incident absorbed photons - 87% - 8.6 μA mA^{-1}
2) diffusely reflected photons - 10% - 1.0 μA mA^{-1}
3) specularly reflected photons - 3% - 0.3 μA mA^{-1}

The very low current produced by specularly reflected photons indicates a high surface roughness. Using the current collected by the pick up wire W in Fig 1 we estimate that diffusely scattered photons are distributed along the entire circumference of the tube. Comparing the normal with 100 mrad photoelectron production reveals a factor of 3 increase for 100 mrad photons which is in good agreement with the data in Fig 11, Ref 3. It also provides a further proof that desorption (PSD) is caused by photo electrons. When the sample is grounded, ~75% of all electrons produced leave the bar and strike the surrounding stainless tube. The substained desorption reported in the next section is therefore due to neutral molecules leaving stainless steel. Assuming the model in Ref 1, i.e., each photoelectron desorbs twice, once on leaving and once on returning to the surface, when the photons first strike the surface about 65% of the desorbed gas comes from the sample and about 35% from the surrounding stainless steel. Once the sample has been exposed to approximately 10^{22} photons per meter practically no gas is desorbed from its surface.

In the following measurements the samples were grounded to the chamber and the currents due to absorbed photons (grazing angle = 100 mrad) were obtained from the wire calibrated in the previous run. Photocurrents produced in the baked(B) and glow-discharged (GDC) samples by a 10 mrad beam are summarized in Table I. Also included are the currents generated in the last column. Inspecting Table I reveals the following facts:

1) Relative photoyields are in good agreement with the calculated valuse for normal incidence

2) Photoyields for GDC samples are lower due probably to increased surface roughness caused by argon sputtering

3) Carbon films absorb almost all photons

4) Photoelectron production at 100 mrad is 4 times larger than that at normal incidence

B. Photodesorption

Two fundamental quantities necessary for vacuum system design are the desorption coefficient, η, and the total gas which must be removed from the surface to obtain a reasonable beam lifetime. Both quantities are plotted vs. photon dose in Figs. 2 through 8, for each run described in section II B. A dramatic improvement takes place after argon glow discharge when the entire surface of the apparatus has been cleaned. From these figures we make the following observations:

1) Sawtoothed copper exhibits the lowest desorption yields because the photons strike the surface at normal incidence. This advantage might not, however, be implemented in high current rings, due to inadequate cooling of the ridges.

2) Carbon ("diamond film") coated and gold plated samples are the next best candidates, but gold plating is much easier. A diffusion barrier must be interposed between Cu and Au.

3) The entire apparatus (Fig 1) was glow discharge for the first time when the Cu bar was being measured and larger quantities of gases were covering its surfaces, than in subsequent runs. Hence, larger amounts of CO and CO^2 were desorbed. All subsequent runs including unreported electrically isolated Cu bar (III A) show smaller total gas desorbed.

4) GDC is very effective in removing CO^2.

IV Discussion

Taking into account the data on photoelectron production (III A) the resulting desorption yields plotted in Figs. 2-7 (III B) can be well understood. While the initial ηS are indicative of the gases on the sample bar, as the photon exposure continues, ηS are more and more governed by gases desorbed from surrounding surfaces. Extending this model to storage rings explains the very large initial gas bursts lasting a few tenths of an Ampere-hour. During this time, the strips of the vacuum chamber exposed to direct photons generated by circulating electrons, are cleaned. Following this burst, a much longer time is required to scrub the entire chamber either by the electrons produced by absorbed photons in the narrow strip or by reflected photons in the rest of the chamber. The amount of desorbed gas per photon is therefore governed by the photoelectric quantum efficiency of the material, the angle of incidence, the reflectivity and the achievable surface cleanliness.

V. Conclusions

Based on the calculations and the measured data we draw the following conclusions pertinent to storage rings:

1) Despite the similar calculated total photoelectron production for Cu, Au and SS, integrated over the photon energies in our experiment, the SS yield is almost three times lower (Table I.). This may suggest a rather rough surface, i.e., most photons hit the surface at much larger angles.

2) Of the 4 smooth metallic surfaces (Be, Cu,, Au, and SS) exposed at 100 mrad incidence, gold-plated copper gives the lowest PSD yield, yet its photoelectron yield is the highest (Table I.). Au surface must therefore contain less total

adsorbed gases than other metals (compare Figs. 2-5) and would be a good candidate for storage ring vacuum chambers.

3) Diamond films are suitable as absorbers. However, more studies are needed on the durability of these films.

4) The discrepency between solid Cu yields reported here and plated Cu yields[6,7] cannot be explained by differences in surface roughness or photoelectron production . A long 300° bake might have significantly lowered the PSD yield.

5) Both the photoelectron production and PSD depend on the angle of incidence and are in good agreement with Fig. 11 Ref. 5

6) Sawtoothed copper is the best choice for long absorbers provided that the synchrotron radiation power does not significantly raise the temperature of the teeth and the impedance. Gold plating would further lower the PSD, but a barrier has to be interposed between Cu and Au due to gold diffusion into copper. Nickel, a common barrier, may not be compatible with magnetic field. Allowing gold diffusion during initial ring conditioning may also be acceptable.

7) A dull finish produces less specular reflection, which is desirable. A gold plate over rough finished copper should result in reduced reflection.

Acknowledgments

The authors would like to thank E. Gaudet and the NSLS Vacuum Group for their excellent support. Assistance given by the NSLS operations crew is also gratefully acknowledged.

References

1. E.L. Garwin, 3 BeV Colliding Beam Vacuum System, SLAC Memorandum, 9/14 1963.
2. T. Kobari and H.J. Halama, J.Vac. Sci. Technol. A5, 2355 (1987)
3. O. Grobner, A.G. Mathenson, P. Strubin, E. Alge and R. Souchet, J. Vac. Sci. Technol. A7, 223 (1989).
4. H. Halama submitted to J. Vsc. Sci Technol (1991)
5. O. Grobner, A.G. Mathenson, R. Souchet, H. Stori and P. Strubin, Vacuum 33(7), 397 (1983).
6. H.J. Halama and C.L. Foerster, Vacuum 42 (3), 185 (1991)
7. C.L. Foerster, H. Halama and C.Lanni, J. Vac. Sci. Technol. 8A, 2856 (1990)
8. C.L. Foerster and G.Korn AIP Proceeding
9. R.H. Day, P. Lee, E.B. Saloman and D.J. Nagel, J. Appl. Phys 52, 6965 (1981)
10. J. Winter, J. Nucl. Matter, 145-147, 131 (1987)
11. J. Winter, F. Waelbroeck, P. Wienhold, Proc 12th SOFT Julich, 369 (1982)
12. Film measurements were performed by A. Tobin Grumman Research Center
13. H.C. Hseuh, J. Vac. Sci. Technol. A3, 518 (1985)
14. H. Halama, AIP Proceedings No 199, 93 (1989)
15. R.A. Mack, Int. Report CEAL 1027, Cambridge Electron Accelerator (1966)

Table I. Sample Bar and Beam Stop Photocurrents in $\mu A/mA$

	Sample		Beam Stop				Diffuse Reflection	
Material	B	G DC	B(I)	B(%)	G DC(I)	G DC(%)	B	G DC
Cu	9.4	6.8	0.87	8.5	0.98	12.5	1	
Au	10.0	7.8	0.65	6	0.53	6	0.7	0.65
Be	7.3	6.3	0.8	10	0.58	9	0.3	0.2
C	4.3	~3	0.03	0.7	0.02	0.7	0.2	0.1
Sawtooth Cu	2.2	1.6	0.007	0.3	0.005	0.3	0.01	0.01
SS	3.3	2.3	0.02	0.6	0.02	0.9	0.01	0.01

Figure Captions

Fig. 1. Schematic diagram of the sample chamber set up and the horizontal off axis layout. (a) Components: 01 - Rectangular conductance; SP - Spool piece; B - Bellows. (b) Layout of sample horizontally on the pivot point. Specucalar photon strike the photon stop.

Fig. 2. Molecular desorption yields and total gas desorbed for OF-copper after bake (Run 1) and after glow discharge conditioning (Run 2).

Fig. 3. Molecular desorption yields and total gas desorbed for gold plated copper after bake (Run 3) and after glow discharge conditioning (Run 4).

Fig. 4. Molecular desorption yields and total gas desorbed for beryllium plates after bake (Run 5) and after glow discharge conditioning (Run 6).

Fig. 5. Molecular desorption yields and total gas desorbed for carbon coating. After bake (Run 7) and after glow discharge conditioning (Run 8).

Fig. 6. Molecular desorption yields and total gas desorbed for sawtooth OF - copper after bake (Run 9) and after glow discharge conditioning (Run 10).

Fig. 7. Molecular desorption yields and total gas desorbed for stainless steel after bake (Run 12) and after glow dischage conditioning (Run 13).

Fig. 8 Molecular desorption yields and total gas desorbed for gold plates copper after bake of previous air exposure following glow discharge conditional in a separate chamber.

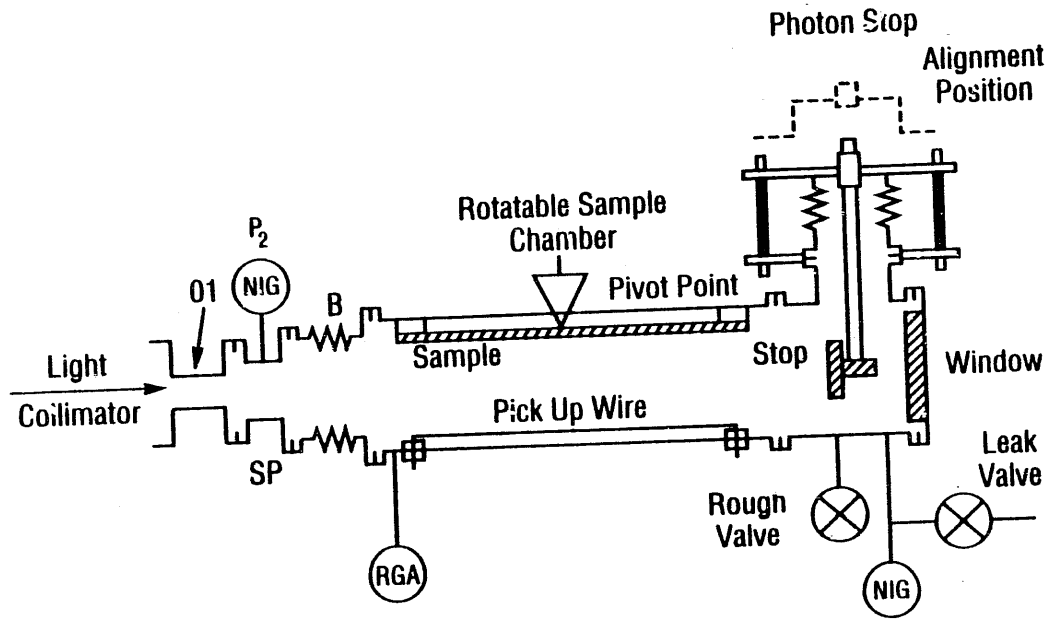

Test Set Up #2

(a)

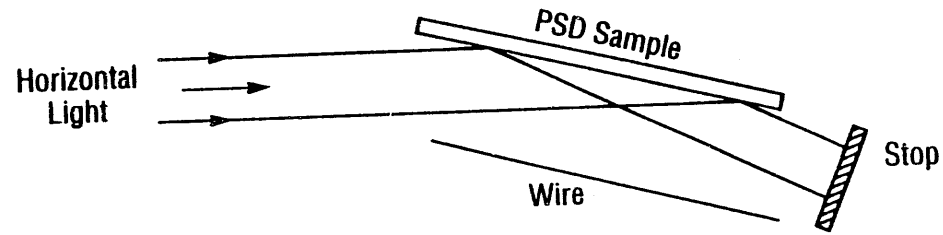

Rotated Sample

(b)

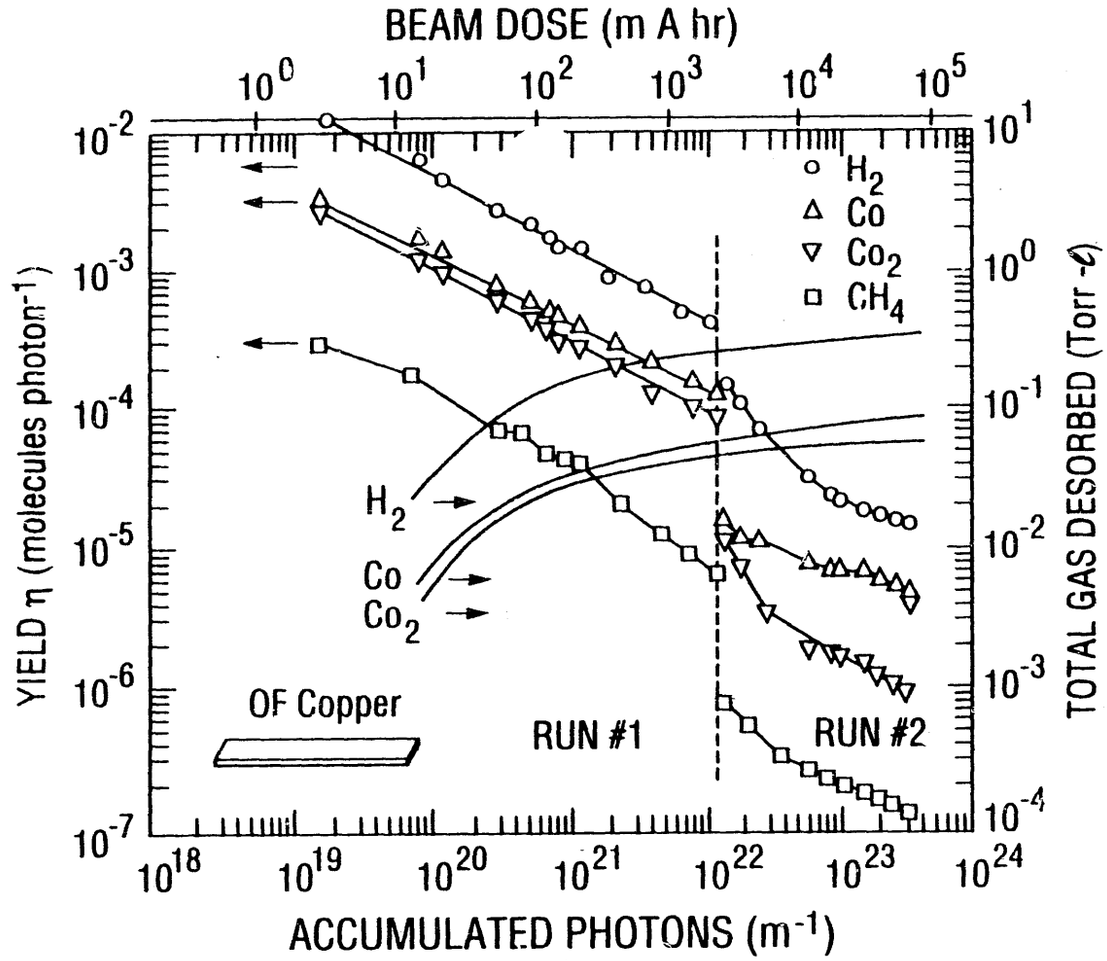
BEAM DOSE (m A hr)
10^0 10^1 10^2 10^3 10^4 10^5
10^{-2} 10^{-3} 10^{-4} 10^{-5} 10^{-6} 10^{-7}
YIELD η (molecules photon^{-1})
10^1 10^0 10^{-1} 10^{-2} 10^{-3} 10^{-4}
TOTAL GAS DESORBED (Torr -ℓ)
H_2
Co
Co_2
CH_4
H_2
Co
Co_2
OF Copper
RUN #1
RUN #2
10^{18} 10^{19} 10^{20} 10^{21} 10^{22} 10^{23} 10^{24}
ACCUMULATED PHOTONS (m^{-1})

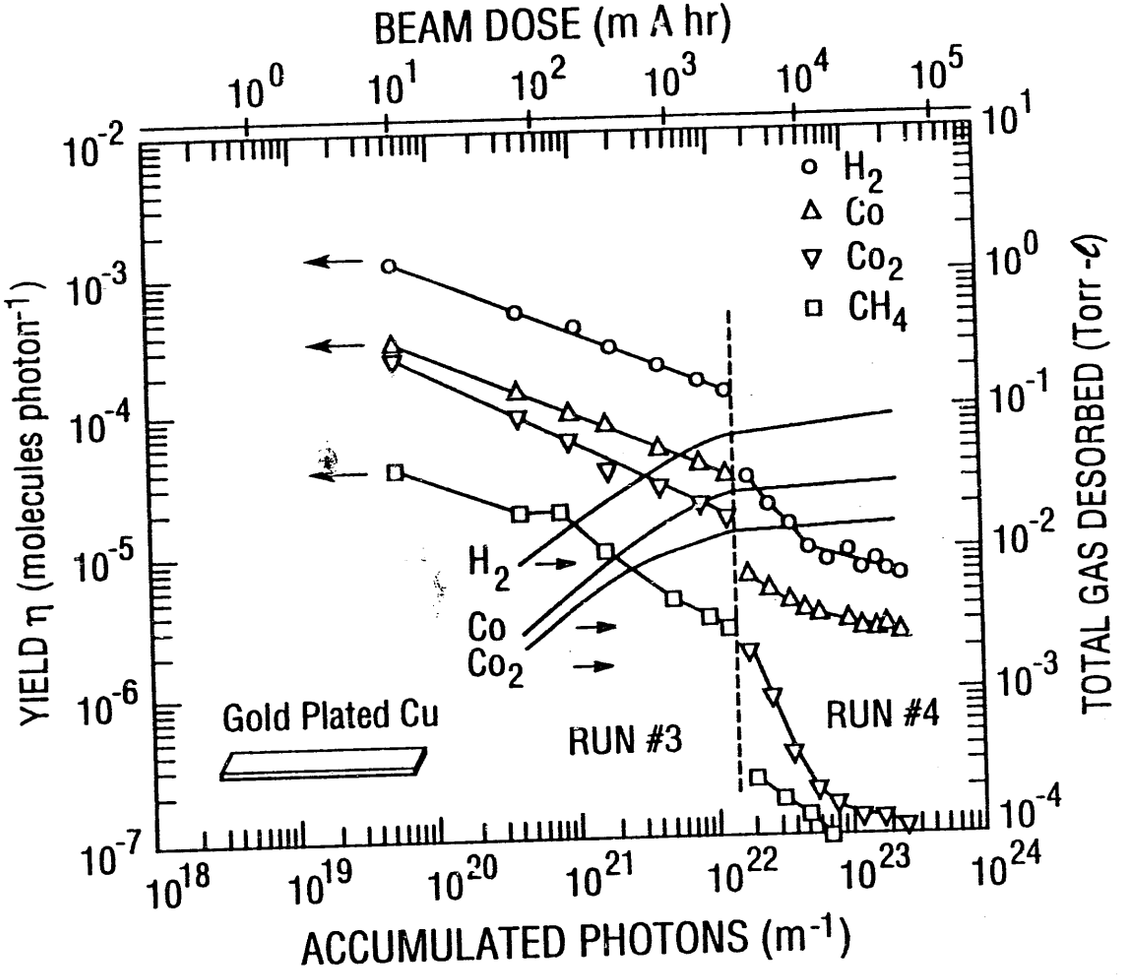
BEAM DOSE (m A hr)
10^0 10^1 10^2 10^3 10^4 10^5
10^{-2} 10^{-3} 10^{-4} 10^{-5} 10^{-6} 10^{-7}
YIELD η (molecules photon^{-1})
10^1 10^0 10^{-1} 10^{-2} 10^{-3} 10^{-4}
TOTAL GAS DESORBED (Torr -ℓ)
H_2
Co
Co_2
CH_4
H_2
Co
Co_2
Gold Plated Cu
RUN #3
RUN #4
10^{18} 10^{19} 10^{20} 10^{21} 10^{22} 10^{23} 10^{24}
ACCUMULATED PHOTONS (m^{-1})

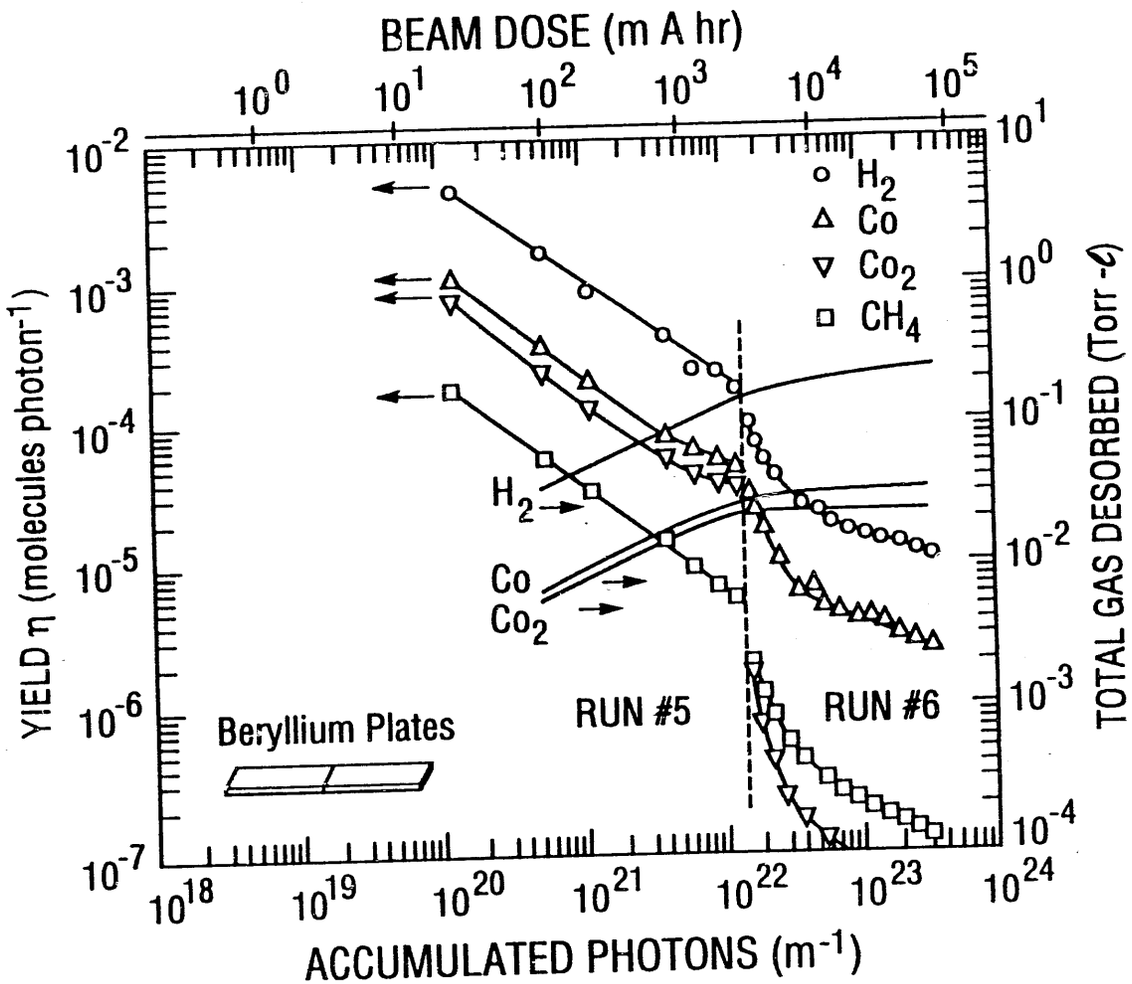
BEAM DOSE (m A hr)
10^0 10^1 10^2 10^3 10^4 10^5
10^{-2} 10^{-3} 10^{-4} 10^{-5} 10^{-6} 10^{-7}
YIELD η (molecules photon^{-1})
10^1 10^0 10^{-1} 10^{-2} 10^{-3} 10^{-4}
TOTAL GAS DESORBED (Torr - ℓ)
H_2
Co
Co_2
CH_4
H_2
Co
Co_2
Beryllium Plates
RUN #5
RUN #6
10^{18} 10^{19} 10^{20} 10^{21} 10^{22} 10^{23} 10^{24}
ACCUMULATED PHOTONS (m^{-1})

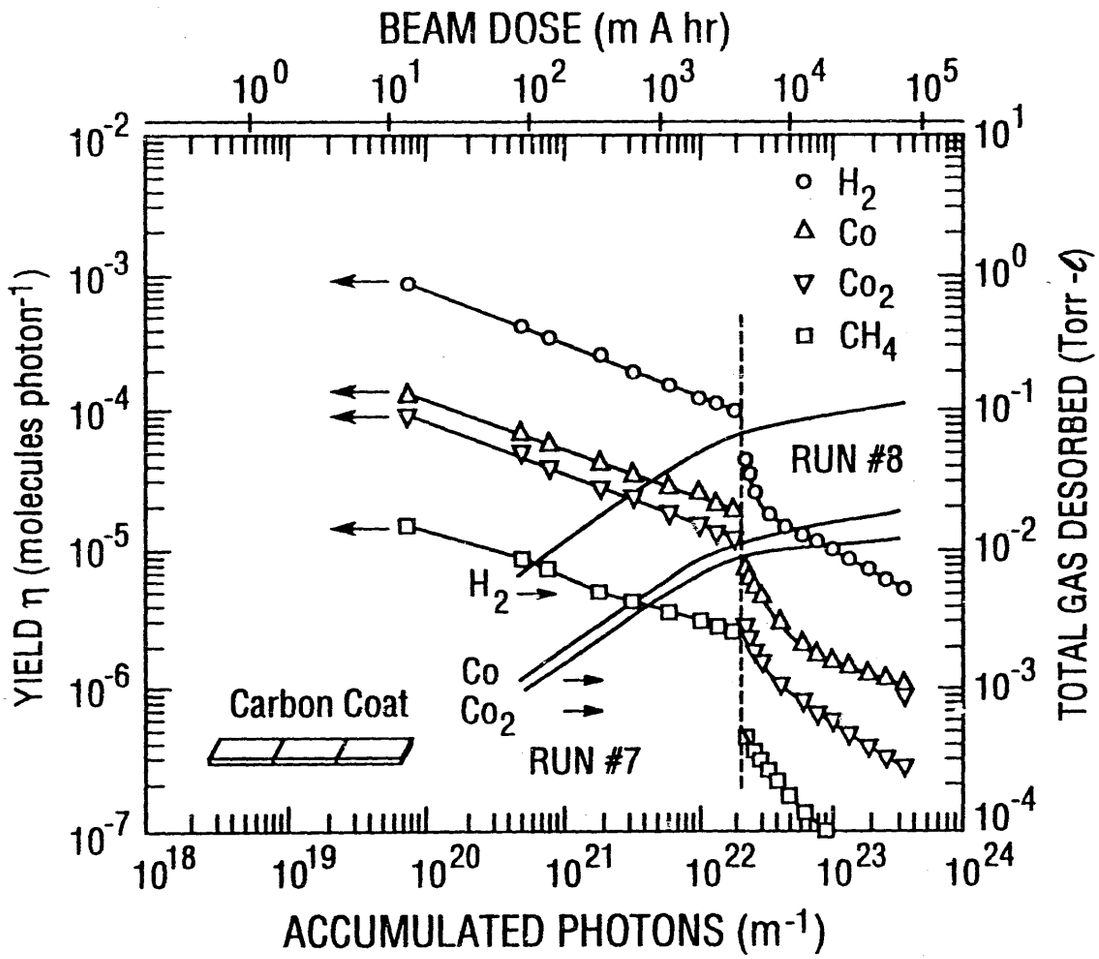
BEAM DOSE (m A hr)
10^0 10^1 10^2 10^3 10^4 10^5
10^{-2} 10^{-3} 10^{-4} 10^{-5} 10^{-6} 10^{-7}
YIELD η (molecules photon^{-1})
10^1 10^0 10^{-1} 10^{-2} 10^{-3} 10^{-4}
TOTAL GAS DESORBED (Torr -ℓ)
H_2
Co
Co_2
CH_4
RUN #8
H_2
Co
Co_2
Carbon Coat
RUN #7
10^{18} 10^{19} 10^{20} 10^{21} 10^{22} 10^{23} 10^{24}
ACCUMULATED PHOTONS (m^{-1})

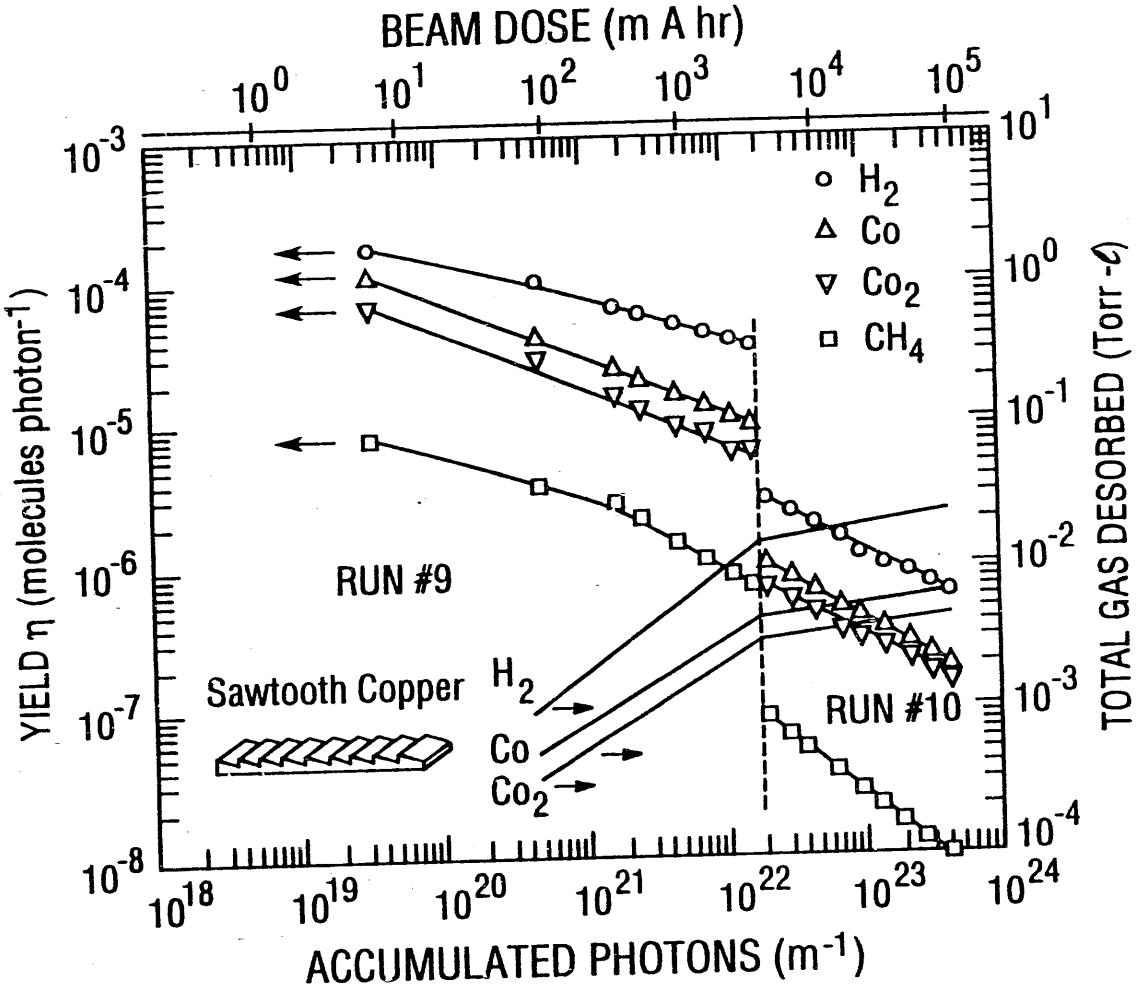

Foerster 4a 9/4/91 j.o.

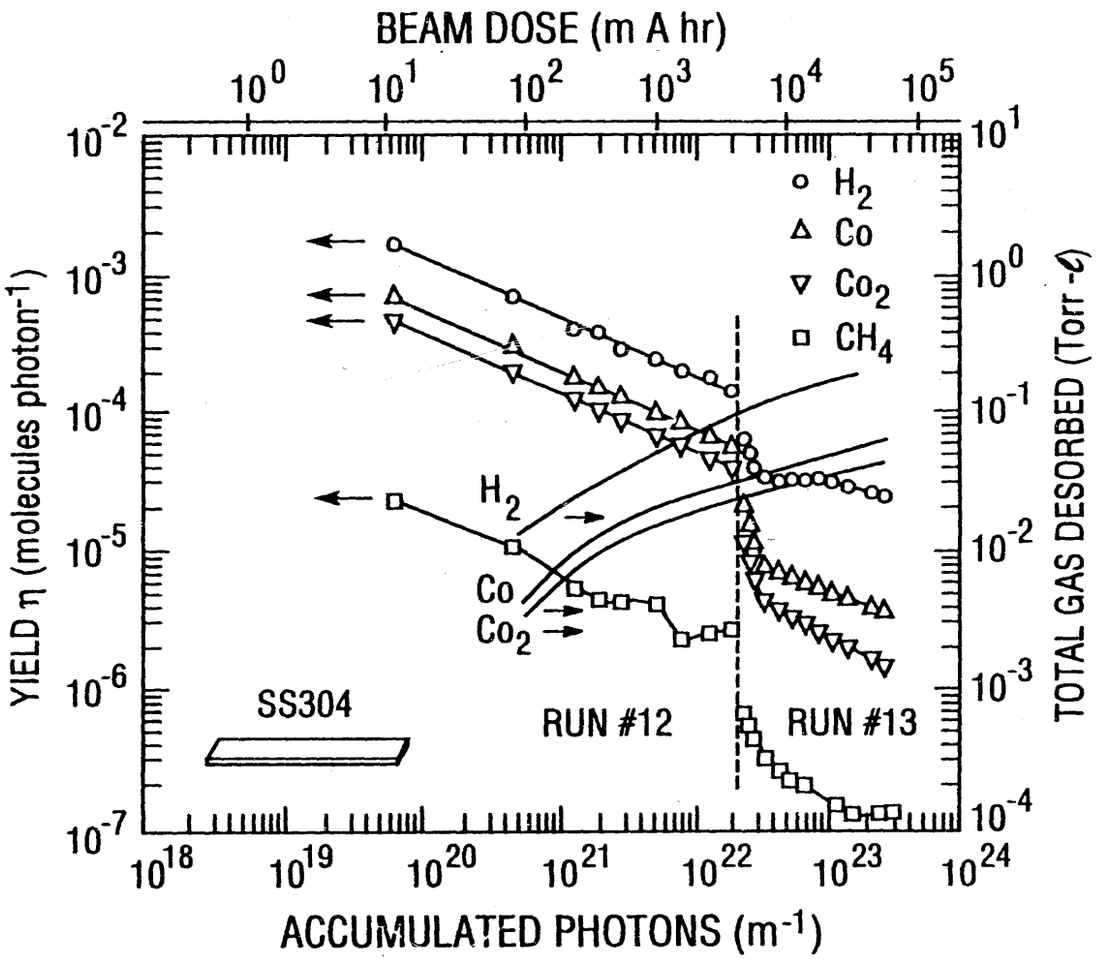
BEAM DOSE (m A hr)
10^0 10^1 10^2 10^3 10^4 10^5
10^{-2} 10^{-3} 10^{-4} 10^{-5} 10^{-6} 10^{-7}
YIELD η (molecules photon^{-1})
10^1 10^0 10^{-1} 10^{-2} 10^{-3} 10^{-4}
TOTAL GAS DESORBED (Torr -ℓ)
H_2
Co
Co_2
CH_4
H_2
Co
Co_2
SS304
RUN #12
RUN #13
10^{18} 10^{19} 10^{20} 10^{21} 10^{22} 10^{23} 10^{24}
ACCUMULATED PHOTONS (m^{-1})

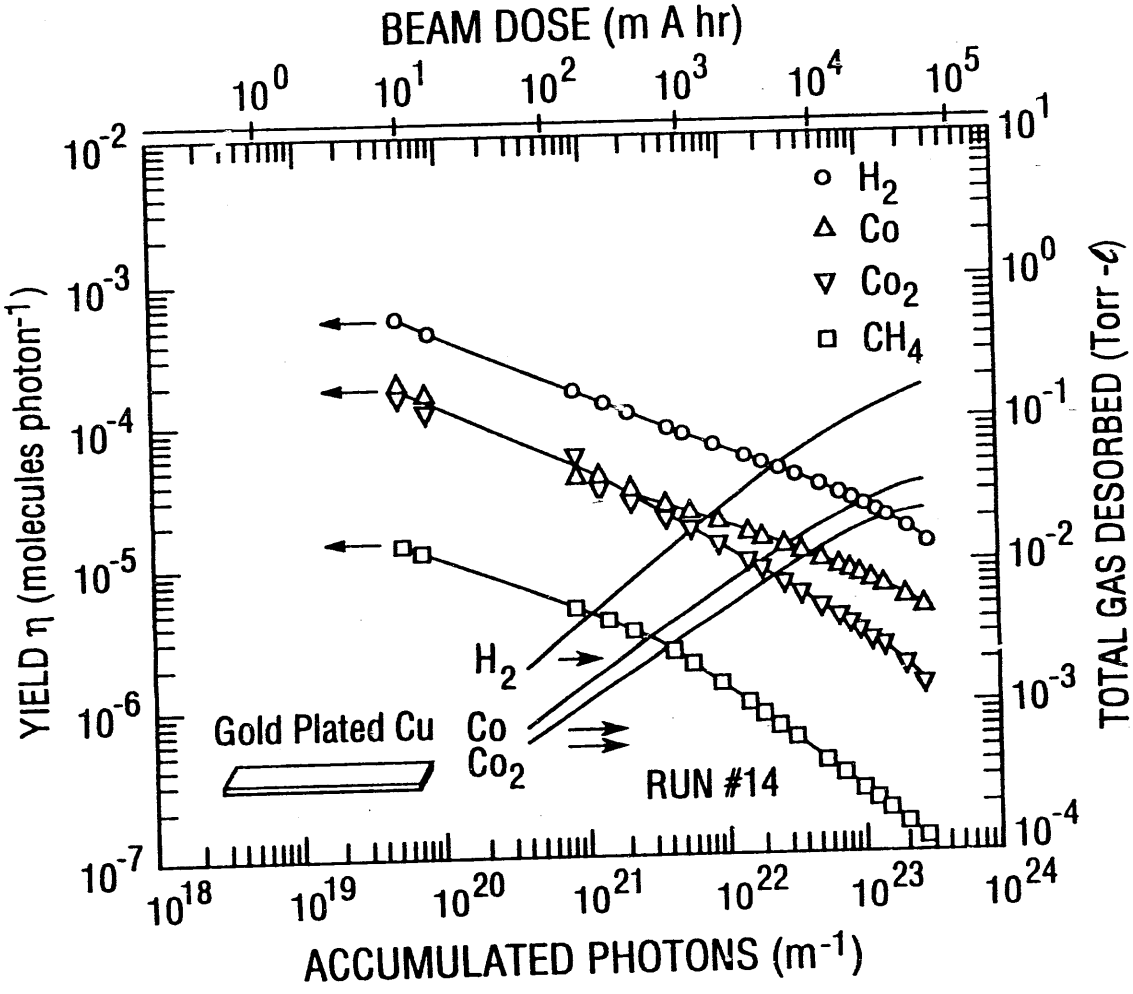
BEAM DOSE (m A hr)
10^0 10^1 10^2 10^3 10^4 10^5
10^{-2} 10^{-3} 10^{-4} 10^{-5} 10^{-6} 10^{-7}
YIELD η (molecules photon^{-1})
10^1 10^0 10^{-1} 10^{-2} 10^{-3} 10^{-4}
TOTAL GAS DESORBED (Torr -ℓ)
H_2
Co
Co_2
CH_4
H_2
Gold Plated Cu
Co
Co_2
RUN #14
10^{18} 10^{19} 10^{20} 10^{21} 10^{22} 10^{23} 10^{24}
ACCUMULATED PHOTONS (m^{-1})

END

DATE FILMED

3/17/92